IEEE Access
Multidisciplinary | Rapid Review | Open Access Journal

Received July 24, 2019, accepted July 26, 2019, date of publication August 8, 2019, date of current version August 21, 2019.

Digital Object Identifier 10.1109/ACCESS.2019.2933834

Mode Composite Coplanar Waveguide

YIHONG SU, XIAN QI LIN, (Senior Member, IEEE), JIA WEI YU, AND YONG FAN, (Senior Member, IEEE)

EHF Key Laboratory of Science, School of Electronic Engineering, University of Electronic Science and Technology of China, Chengdu 611731, China

Corresponding author: Xian Qi Lin (xqlin@uestc.edu.cn)

This work was supported in part by the NSFC under Grant 61571084, in part by the Equipment Pre-Research Funding (EPRF) under Grant 6141B06120101, and in part by the National Department Science and Technology Innovation (NDSTI) under Grant 1716313ZT00802902.

ABSTRACT In this paper, a mode composite coplanar waveguide (MCCPW) is proposed and studied. The MCCPW can be regarded as a combination of a quasi-coplanar waveguide and a substrate integrated waveguide (SIW). In this composite structure, the center conductor of the quasi-coplanar waveguide serves as the SIW supporting TE_{10} mode, while the TEM mode operates in the quasi-coplanar waveguide part. The characteristics and design method of the MCCPW are analyzed and illustrated in this work. The MCCPW is fabricated together with two transition structures to demonstrate its integration capability further with other planar circuits. The MCCPW is a single layer structure, and it has the advantages of joint structure and mode composition, which make it a possible solution for multifunction and multiband application systems. The measured and the simulated results agree well with each other, and good transition performances are achieved.

INDEX TERMS Mode composite coplanar waveguide (MCCPW), multiband, quasi-coplanar waveguide (QCPW), substrate integrated waveguide (SIW), structure sharing, TE_{10} mode, TEM mode.

I. INTRODUCTION

With the rapid development of microwave wireless communication systems, there are much demands of compact size high-performance microwave circuits with broadband and multiband functionalities. Mainly, in the emerging fifth-generation (5G) wireless communication system, the operating frequency can be located at 28GHz, 35GHz, and even up to 57-71GHz. So there will be a large frequency ratio between the present and the forthcoming wireless communication systems as the present one covers the frequencies up to 6GHz. Therefore, one of the speculated technologies in future systems is to integrate the low and high-frequency circuits or antennas to minimize the overall size of the system.

For passive microwave circuits and antenna design, the interference from the adjacent circuits and the mutual coupling caused by the surrounding antenna element impede the miniaturization of the microwave system. Hence, it exists a high demand for the passive circuit with joint structure and antenna with shared-aperture achieve the size reduction while maintaining the performance of the original system in the meantime.

The associate editor coordinating the review of this manuscript and approving it for publication was Giorgio Montisci.

Due to the above concern, a mode composite waveguide is proposed and demonstrated in [1]. The MCW consists of an inner rectangular metallic structure and outer rectangular metallic enclosure. The inner conductor works as an SIW supporting high-frequency signals and the outer enclosure together with the outside surface of the inner conductor work as the substrate integrated coaxial line supporting TEM mode.

The structure of the MCW involves naturally physical isolation by using the substrate integrated waveguide (SIW) [2]–[8]. The SIW technology is a promising approach used in transmission structures in high-frequency microwave circuits design for its high-power capacity, low losses, simple structure, and easy integration with other planar circuits. Moreover, multiple microwave circuits and antennas can be achieved by utilizing the SIW structure. Hence, it is reasonable to come up with a new concept that combines SIW and other transmission lines with structure sharing and mode composite characteristics.

However, for the present MCW designs, the multilayer PCB process increases its difficulty in integrating with other planer circuits, and it is challenging to use the SIW part of the MCW for the antenna design due to the shielding structure of substrate integrated coaxial line. Thus, it occurs to the researchers to design a single layer planar transmission line

to expose the SIW to the air. In this case, the transmission line can be used for both microwave circuit and antenna design. Therefore, a new mode composite transmission line named the dual-mode composite microstrip line (DMCMS) that combines the SIW and microstrip line is proposed, and the SIW is regarded as the thick conductor strip of the microstrip line. Besides, a dual-band leaky wave antenna is presented in [7] which needs two-layer substrates for the transmission line itself. Based on these reasons, a single layer mode composite transmission line is proposed in this paper by combining the SIW and coplanar waveguide (CPW).

The CPW configuration is an ideal candidate for use with surface mounted components [9]–[11]. The impedance of the coplanar waveguide can be adjusted flexibly by controlling the value of multi-parameters to meet different system requirements. The microwave power is constrained in the slot between the center conductor and the ground, and it can be used to design slot antenna since the coplanar waveguide is an open structure. Unlike the SIW that naturally has a cutoff frequency; the bandwidth of coplanar waveguide transmission covers both low and high frequency. This feature can tackle the weakness of the SIW in low-frequency application.

The SIW and CPW are complementary to each other. Therefore, combining the two-waveguide structures to design a new transmission line becomes a reasonable choice. It is the original idea of the proposed mode composite coplanar waveguide (MCCPW).

The unique advantages of the MCCPW are concluded as follows (which will be demonstrated in the following sections): The mode composite coplanar waveguide will possess the characteristics of structure sharing and high mode isolation due to the enclosing structure of the SIW. These characteristics will lead to size reduction and high design freedom in future microwave circuits and antennas, especially in multi-band application. Besides, the inherited advantages of the SIW structure, the single layer topology of the MCCPW makes it easy to integrate with other planar circuits and decrease the fabrication difficulty as well.

In this paper, section II introduces the structure of the proposed MCCPW. Section III presents the characteristics of the MCCPW including the characteristic impedance and complex propagation constant. Section IV and V present two feeding techniques of MCCPW named the joint feeding network and the impedance matching structure respectively. The two types of transition structures broaden the application scenario of the MCCPW and make it easy to integrate with other planar circuits. Then, the simulated and measured results are presented to demonstrate the feasibility of the proposed MCCPW in Section VI. The conclusion is given in section VII which point out the potential application of MCCPW.

II. STRUCTURE AND WORKING PRINCIPLE OF THE MCCPW

The structure of the MCCPW is shown in Fig.1. It is similar to the coplanar waveguide (CPW) containing a center conductor

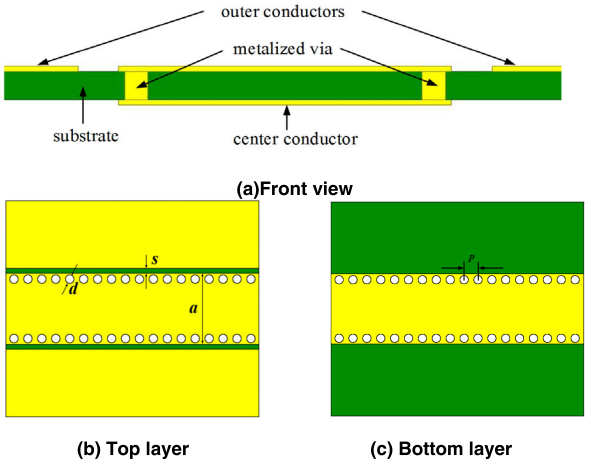

FIGURE 1. Structure of the mode composite coplanar waveguide. (a)Front view. (b) Top layer. (c) Bottom layer.

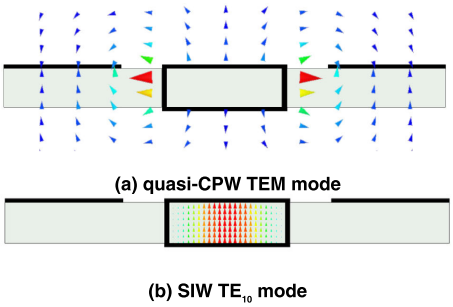

FIGURE 2. Mode distribution of the MCCPW. (a) Quasi-CPW TEM mode. (b) SIW TE 10 mode.

and two outer conductors that lie in the same plane. The difference is that the MCCPW has a thick hollow center conductor which can be regarded as the substrate integrated waveguide (SIW). The thickness of the center conductor is equal to the thickness of the substrate h assuming the surface mounted metal thickness to be zero. The gap between the center conductor and outer conductor and the size of the center conductor jointly determine the characteristic of the CPW part of the MCCPW. The CPW part of the MCCPW is called quasi-CPW (QCPW) in this paper.

The center conductor is endowed with two functions. One is to serve as the center conductor of the QCPW supporting TEM mode, and another is to serve as the SIW supporting TE_{10} mode higher than its cutoff frequency. The cutoff frequency of the SIW is defined as in (1)

$$f_c = \frac{c_0}{2w_{eff}\sqrt{\mu_r \varepsilon_r}}$$
$$w_{eff} = a - d - 1.08\frac{d^2}{p} + 0.1\frac{d^2}{a-d} \quad (1)$$

where c_0 represents the velocity of light in air, d is the diameter of the metal vias, p is their longitudinal spacing, a represents the width of the center conductor, μ_r and ε_r are the relative permeability and relative dielectric constant of the substrate, respectively. The value of a parameter depends on the desired high frequency.

TABLE 1. Comparison of MCCPW with other mode composite transmission lines.

	MCCPW (SIW+QCPW)	MCW [1] (SIW+SICL)	DMCMS [7] (SIW+Microstrip line)
Loss	Low	Medium	Low
Cost	Easy	Medium	Medium
Integration	Easy	Medium	Easy
layer	1	3	2
Radiation	Medium	Low	Medium

The mode distribution of the MCCPW is shown in Fig.2. The TEM mode and TE_{10} mode are supported in the QCPW and SIW parts respectively. It can be noticed that the TEM mode transmitted in the CPW part of the MCCPW has a mono-mode frequency region with the large frequency coverage; this feature is beneficial to the broadband wireless communication system. The MCCPW can be fabricated in a single-layer substrate, which makes it easy to integrate with other planar microwave circuits. Table I presents the comparison of the MCCPW with other types of mode composite transmission line designed previously in [1] and [7].

III. CHARACTERISTICS OF MCCPW

The SIW structure used in MCCPW makes physical isolation between the QCPW TEM and SIW TE_{10} transmission mode. The QCPW and SIW part can be therefore independently designed without electrical interference which largely reduces the design complexity. The parameters of interest for a transmission line are its characteristic impedance and complex propagation constant which contains the phase constant β and attenuation constant α.

A. THE CHARACTERISTIC IMPEDANCE OF MCCPW

When considering the characteristic impedance of the MCCPW, it is better to follow the design standard of the 50Ω system. The impedance range of the SIW and the QCPW part need to be studied for the sake of the subsequent transition to other microwave circuits designs and experiments. Noticing that the outer conductor is assumed to be an infinite conductor plane in an ideal QCPW model which is hard to achieve in real fabrication. In this case, the width of the outer conductor for each side is chosen to be greater than four times the size of the center conductor to decrease the calculation error.

The calculation of the characteristic impedance Z_0 of a microwave transmission line can be turned into the derivations of capacitances C and C_0 using (2)-(4).

$$\varepsilon_r = \frac{C}{C_0} \tag{2}$$

$$v_{ph} = \frac{c_0}{\sqrt{\varepsilon_r}} \tag{3}$$

$$Z_0 = \frac{1}{Cv_{ph}} \tag{4}$$

where C and C_0 represent the capacitance per unit length of the line and the capacitance per unit length of the line when the substrate is replaced by air, v_{ph} is the phase velocity.

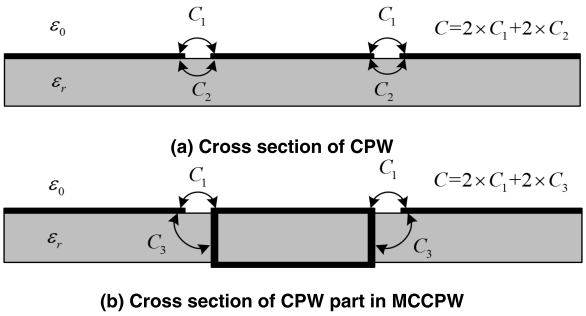

FIGURE 3. Comparison of Capacitance between the CPW and CPW part in MCCPW. (a) Cross section of CPW. (b) Cross section of CPW part in MCCPW.

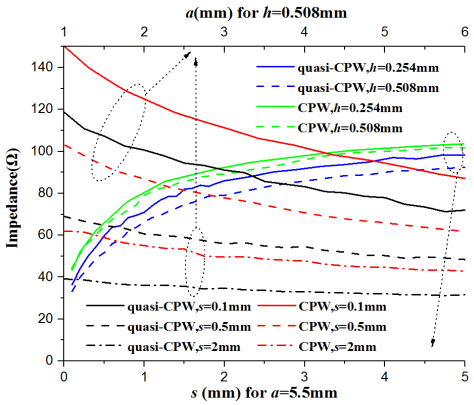

FIGURE 4. Simulated characteristic impedance of the CPW part at different substrate thicknesses and slot widths. ($\varepsilon_r = 2.2$, $f = 3.5$GHz).

The traditional method for the calculation of C is based on the conformal mapping method to transfer the complex structure to a simple calculated structure and then using the known equation to get the precise value of C, but it is hard to get an analytical expression of CPW part of MCCPW using conformal mapping method in this case. However, we can conclude that with the same size of QCPW and traditional CPW, the characteristic impedance of QCPW is less than traditional CPW. It can be obtained by qualitative analysis as shown in Fig.3. The value of C_3 is larger than the value of C_2 due to the large size of the coupling area. This means that the CPW part in MCCPW can achieve a lower characteristic impedance easily considering the minimum length of slot width beside the CPW center conductor in real fabrication.

In this paper, the characteristic impedance of the MCCPW is extracted using the EM software HFSS which is efficient and accurate. As shown in Fig.4, the impedance of the QCPW is proportional to the s and reversely proportional to a. The variation trend is similar to a traditional CPW structure.

The characteristic impedance of the SIW part of the MCCPW is the same as the traditional SIW. Its characteristic impedance is presented in Fig.5 which is proportional to h and inversely proportional to a. The characteristic impedance of the SIW is high and dispersive near the cutoff frequency and tends to be stable in its higher frequency. So some margin needs to be left during its design. Furthermore, the mono-mode frequency range should be taken into consideration

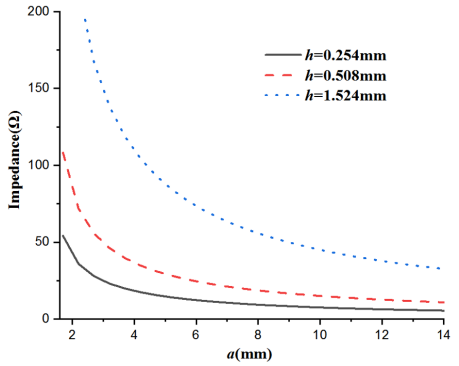

FIGURE 5. Simulated characteristic impedance of the center conductor SIW part at different substrate thicknesses and SIW widths. ($d = 0.4$mm, $\varepsilon_r = 2.2$, $f = 50$GHz).

in its practical design. This feature has been widely studied in [12].

B. THE COMPLEX PROPAGATION CONSTANT OF MCCPW

Besides the impedance of the MCCPW, the phase constant β and the attenuation constant α are essential factors in evaluating the characteristic of a transmission line. Both parameters can be obtained using eigenmode solver in electromagnetic simulation software CST for waveguiding structures. The phase constant β can be calculated by the following equations for TEM and TE_{10} mode respectively.

$$\beta = \frac{2\pi}{\lambda_g} \tag{5}$$

$$\lambda_g = \frac{c_0}{f\sqrt{\varepsilon_r \mu_r}} \quad \text{for TEM mode} \tag{6}$$

$$\lambda_g = \frac{2\pi}{\sqrt{\frac{\varepsilon_r (2\pi f)^2}{c_0} - \left(\frac{\pi}{a-2d}\right)^2}} \quad \text{for } TE_{10} \text{ mode} \tag{7}$$

where λ_g is the guided wavelength, c_0 represents the velocity of light in air, a represent the width of the center conductor, d is the diameter of the SIW sided metallic vias, μ_r and ε_r are the relative permeability and relative dielectric constant of the substrate, respectively.

The QCPW supports the TEM mode as its fundamental mode, so the guided wavelength λ_g is in linear proportion with the frequency as shown in (5). For the SIW part, the fundamental mode is TE_{10} mode, and the guide wavelength λ_g will follow the (6). The calculated result is shown in Fig.6.

The attenuation constant α is taken into concern and calculated by the (8) [13]. It indicates the losses in the MCCPW.

$$\alpha = \left(\frac{\omega_0}{v_g}\right)\left(\frac{1}{2Q}\right) \tag{8}$$

where ω_0 is the angular frequency, $v_g$is the group velocity, and Q is the quality factor of the proposed transmission line structure. The calculated results are shown in Fig.7 and Fig.8.

For the QCPW, the attenuation increases slowly with frequency, and in a certain frequency, the losses are proportional to the parameter s and inversely proportional to a. It is the same variation trend with the characteristic impedance which means that the losses will decrease as the impedance of the QCPW decreases. It is found that the attenuation in QCPW is less than the traditional CPW structure due to its lower characteristic impedance under the same parameter.

For the SIW part, the attenuation constant is high around the cutoff frequency and tends to be stable in

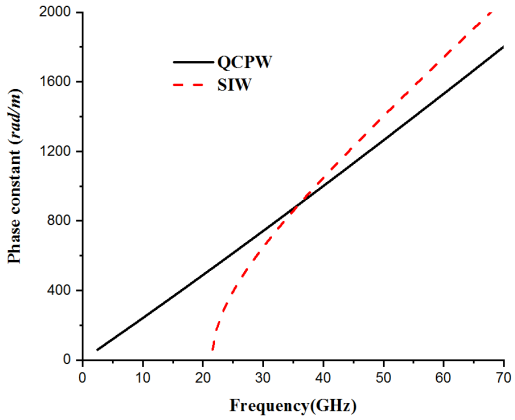

FIGURE 6. Calculated phase constant for SIW part and QCPW part of MCCPW, for $h = 0.508$mm, $s = 0.3$mm.

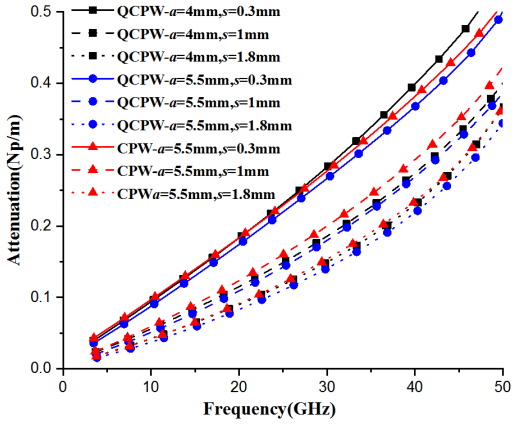

FIGURE 7. Calculated attenuation constant for QCPW structure, for $h = 0.508$mm.

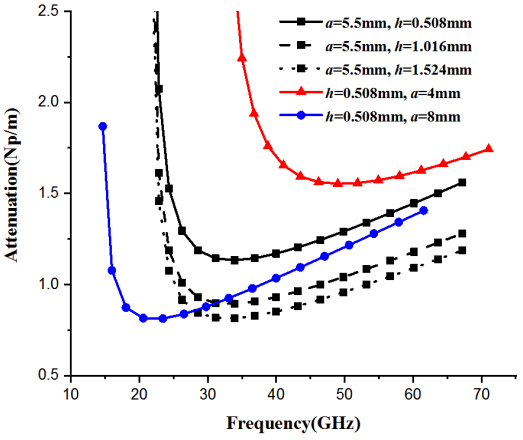

FIGURE 8. Calculated attenuation constant for SIW part of MCCPW.

higher frequency. The calculated losses are higher than the QCPW under the ideal model that the roughness of the metal is not taken into concern. The dielectric losses play the primary role in the total losses in this case. But the high conductor losses will significantly deteriorate the transmission performances in mm-wave application. For the SIW, the attraction lies in that the amount of metal carrying the signal is far greater than what it would be in microstrip or CPW. Therefore, the conductor loss is lower. And since the SIW is an enclosure structure, it has lower radiation losses as compared to other planar transmission lines like CPW and microstrip line, those losses are prominent in mm-wave (even higher) circuit especially in the discontinuity region. Hence, it is suitable for SIW part in MCCPW in the high-frequency application.

C. DESIGN STEP

To achieve the optimal impedances for both the SIW and CPW part of the MCCPW, the design of characteristic impedance should be based on the following steps.

Step 1: Determine the width a and the substrate material with the relative dielectric constant ε_r of the center conductor based on the cutoff frequency of the SIW according to (1) and make sure that the cutoff frequency f_c and the desired frequency band have enough margins. Because the characteristic impedance is unstable with a sharp decrease skirt near the cutoff frequency and it tends to be an approximate constant in higher frequency.

Step 2: use Fig.4 to get the initial value of s, and use the electromagnetic simulation software to get a precise value of the characteristic impedance of the QCPW. In this case, to obtain 50Ω impedance for QCPW, the value of s is chosen to be 0.43mm.

The substrate used in this paper is of type Rogers RT/duroid 5880 with the permittivity constant value of 2.2. The substrate thickness is chosen to be 0.508mm for the standard fabricating size. The above design procedure and characteristic analysis can help the reader to better understand and design MCCPW within a short time by combining the theoretical equations and electromagnetic simulations.

To demonstrate and testify the performance of the MCCPW, two types of transition structures are designed and analyzed. Also, the transition structure is needed when integrating MCCPW with other microwave transmission lines or circuits in practical use. The following transition structures can achieve two different functions and can be applied in different scenarios.

IV. JOINT FEEDING NETWORK

A joint feeding network is proposed in this paper to measure the MCCPW using the conventional fixture and demonstrate its integration capabilities with other planar circuits. The QCPW based TEM mode and SIW based TE_{10} mode can be excited separately or simultaneously using the joint feeding network.

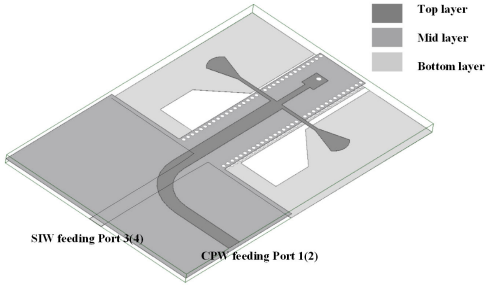

FIGURE 9. Layout of the proposed joint feeding network.

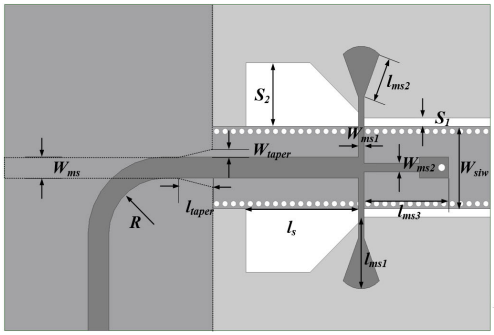

FIGURE 10. Structural parameters of proposed joint feeding network (W_{ms} = 1.5mm, R = 4mm, l_{taper} = 2.5mm, W_{taper} = 0.1mm, S_2 = 4.5mm, l_s = 8.1mm, S_1 = 0.75mm, W_{ms1} = 0.41mm, W_{ms2} = 0.6mm, l_{ms1} = 5.55mm, l_{ms2} = 3.22mm, l_{ms3} = 6.1mm, W_{siw} = 5.5mm).

The structure of the joint feeding network is shown in Fig.9. It consists of two-layer substrates and three-layer metal surfaces. The SIW feeding microstrip line and CPW feeding microstrip line share the common ground plane, and they are placed on the opposite side of the substrate. Fig.10 lists the main design parameters of the proposed joint feeding network. Traditional tapered microstrip line transition is applied to excite SIW TE_{10} mode [3], [13]–[15]. The microstrip line to QCPW transition is based on two pairs of microstrip to slot line transition. The purpose of the short ended microstrip line is to introduce an extra transmission pole in the desired frequency band, and it will improve the bandwidth of the transition [17]–[19].

For the transition from the microstrip line to QCPW, the parameters W_{ms1} and W_{ms2} are contributed to the matching performance in the cross discontinuity. These parameters will be kept almost unchanged when the transition is designed in a different frequency band. While the parameters l_{ms1} and l_s will determine the working band of the transition, and the parameters S_1, S_2, and $angle_1$ are related to its transition bandwidth. The length of the open-ended microstrip line l_{ms1} from the intersection point to the open-ended point is about a quarter wavelength of the microstrip line, while the length of short ended slot line l_s from the intersection point to the short-ended point is about a quarter wavelength of slot line. The tapered slot line and the sector microstrip line are employed to improve the return loss and therefore decrease the losses caused by the transition.

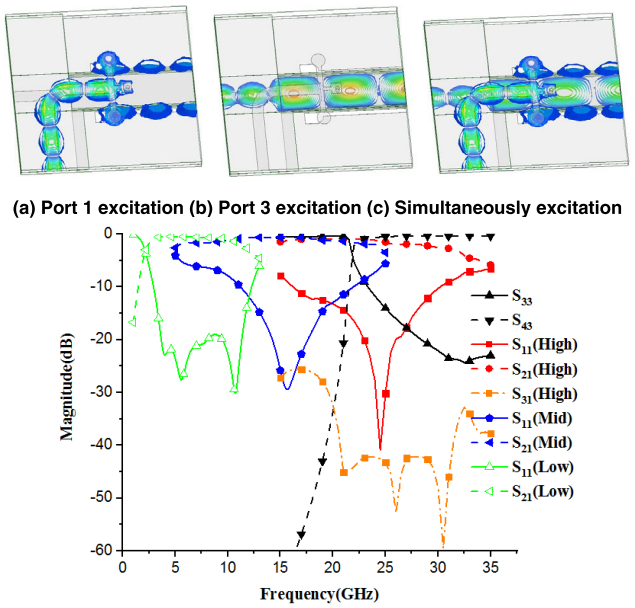

FIGURE 11. Simulated S-parameter of the joint feeding structure (d) and its field distribution in 25GHz. (a) Port 1 excitation. (b) Port 3 excitation. (c) Simultaneously excitation. (d) Simulated S-parameter of the joint feeding structure.

The joint feeding network can excite the two modes independently and simultaneously without affecting each other. Fig.11 shows the simulated result of three joint feeding structures with the same parameter values, namely the W_{taper}, L_{taper}, and W_{siw} in SIW feeding part. Hence, the simulated S_{33} and S_{43} are the same for the three joint feeding structures. Therefore, only one curve is given in Fig.11 to avoid needless duplication. The three joint feeding structures of the QCPW part are designed in different bands to show its design flexibility. The joint feeding structure works in the high band with some overlap with the SIW part. The field distribution at 25GHz is presented in Fig.11 (a) (b) (c), when only port 1 is excited, the MCCPW will support TEM mode in its QCPW part, and the TE_{10} mode will be transmitted in SIW part when port 3 is excited. When port 1 and port 3 are excited simultaneously, the two modes will exist in different parts of the MCCPW. S_{31} is presented in Fig.11 (d) to show the high isolation between the two modes. The joint feeding structure in this paper can avoid the quarter wavelength branch effect compared with [1] because the microstrip to SIW transition terminates before the start point of the QCPW. In this case, the bandwidth is wider than other types of mode composite transmission lines reported in [1] and [7]. The simulated and measured results of the back to back joint feeding network together with the MCCPW are presented in section VI.

V. IMPEDANCE MATCHING STRUCTURE

The joint feeding network can excite the two fundamental modes inside the MCCPW independently and simultaneously so that the two modes can work on their desired frequency bands without affecting each other. While as illustrated in the

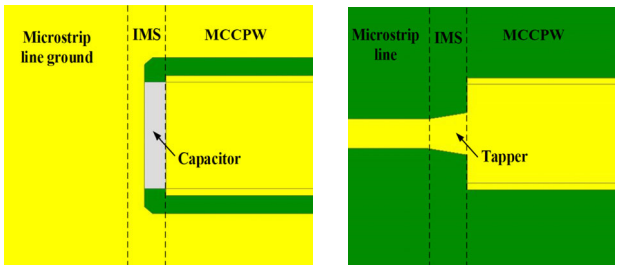

FIGURE 12. Impedance matching structure. (a) Top layer. (b) Bottom layer.

previous section, one of the essential application scenarios of MCCPW lies in the future multiband system such as the 5G communication system. The frequency spectrum for the 5G system consists of the sub-6GHz as its low-frequency band and 28GHz in Ka-band as its high-frequency band. An impedance matching structure from the microstrip line to MCCPW using only a single layer and one feeding port is proposed to meet this kind of requirement.

The Impedance matching structure (IMS) presents the characteristic that the quasi-TEM mode in the microstrip line will transfer to the CPW TEM mode and SIW TE_{10} mode in the desired low and high-frequency band respectively. It requires that the IMS matches different parts of MCCPW and meanwhile excites the corresponding transmission mode. In this case, there is only one feeding port needed, and therefore, the number of the channel in the system is saved.

The difficulty in designing the IMS lies in that for a traditional tapered microstrip line to SIW transition structure [16]–[18], the metalized vias will serve as a shorted stub which makes the electromagnetic wave a total reflection below the cutoff frequency of the SIW. To couple the low-frequency signal from the microstrip line to the coplanar waveguide of the MCCPW, the ground near the junction between the microstrip line and MCCPW must be cut off in the desired low-frequency band. But in the desired high frequency the ground should act like a complete ground. This effect is similar to a capacitor or a high pass filter.

The structure of the proposed IMS is shown in Fig.12 to meet the above consideration. It consists of a conventional tapered line for microstrip line to SIW transition on the up plate, and a gap between the ground plane of the microstrip line and the center conductor of the MCCPW with a lumped capacitor in it. The capacitor prevents the electromagnetic field from shorting to the ground in the low-frequency band and forms an unbroken ground to guarantee the microstrip to SIW transition in the high-frequency band. The filtering skirt of a capacitor is not that sharp compared to the high pass filter, but a capacitor has a smaller size and broadband consistent frequency response. Due to this fact, the desired high-frequency band is usually chosen to be greater than five times the low band frequency for better performance.

The value of the capacitor depends on the frequency gap between the desired low and high frequency. The equivalent circuit of the IMS is shown in Fig.13. We divide the

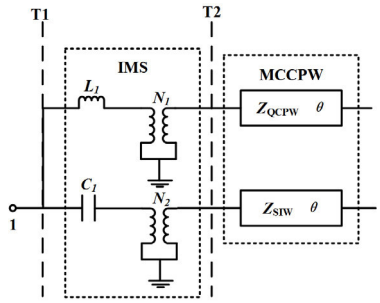

FIGURE 13. Equivalent circuit of the proposed IMS.

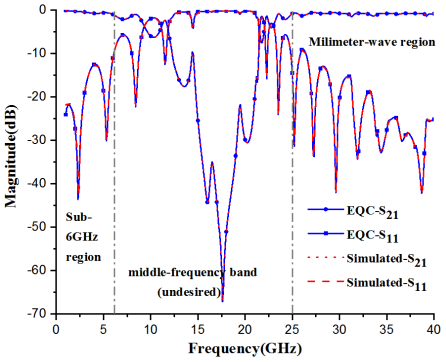

FIGURE 14. Simulation frequency response (ADS) of IMS-MCCPW-IMS back to back equivalent circuit compared with the simulation results in HFSS.

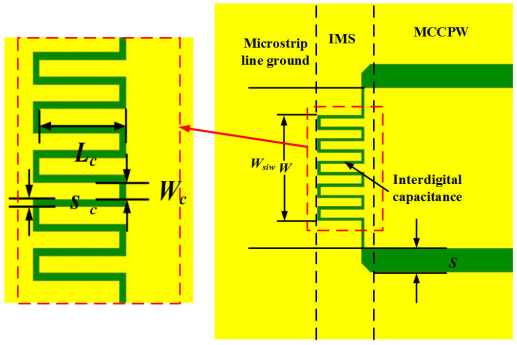

FIGURE 15. The top layer of the IMS topology. ($l_c = 1.2$mm, $w_c = 0.124$mm, $s_c = 0.11$mm, $W_{siw} = 5.43$mm, $s = 0.43$mm).

MCCPW as the QCPW and SIW to represent the two paths. The IMS will work as a frequency dependent switch where the microwave signal will be transferred to different parts of the MCCPW as different modes in its corresponding frequency bands. In the desired low-frequency band, the signal is coupled from the microstrip line to QCPW. This result is similar to an inductance effect. In the high-frequency band, the signal is transferred to SIW, so there will be a series capacitor in the SIW route. The transformer in each path can indicate the impedance mismatching performance between the microstrip line and MCCPW.

The lumped capacitor or chip capacitor used in the IMS is difficult to assemble in the practical application. It is difficult to maintain consistency when soldering the capacitor to the substrate. So, the lumped capacitor used in the early stage of the design is replaced by an interdigital capacitor for the integration. Fig.15 shows a designed IMS for MCCPW integrated with microstrip line to demonstrate the proposed impedance matching structure. The capacitor is replaced by the interdigital capacitor rather than the lumped chip capacitor. In this case, the MCCPW is easy to fabricate and package. Notice that the value of W is less than a parameter in this IMS design for better impedance matching effect. The equivalent circuit and specific parameter design of the interdigital capacitor can be referred to as in [20], [21].

The proposed IMS is verified by the actual model simulated in HFSS. The result in Fig.14 shows a perfect agreement. In sub-6GHz the MCCPW works in QCPW as TEM mode, and in millimeter wave region it works in SIW part as TE_{10} mode. The middle-frequency band is often undesired, though the transition cannot provide a perfect rejection performance in the whole middle-frequency band, it can help to reject some inferences partially. This feature is essential in the future microwave circuits design such as the dual-band filter with large frequency ratio where it can help to suppress some higher mode harmonics efficiently [22], [23].

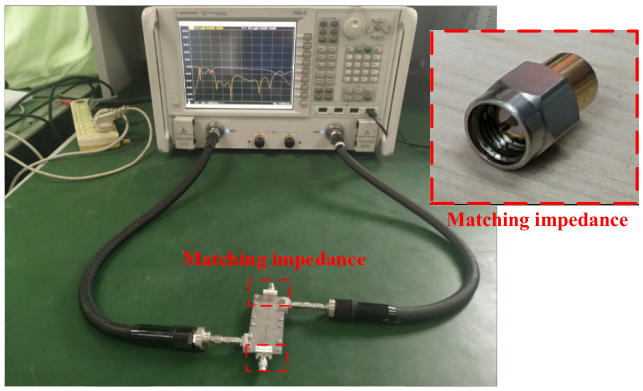

FIGURE 16. Measurement setup of the proposed MCCPW with joint feeding network.

VI. SIMULATION AND MEASUREMENT RESULTS

The measurement setup of the proposed MCCPW with joint feeding network is shown in Fig.16. The choice of the substrate and design dimensions of the MCCPW is based on a tradeoff in impedance matching within the desired operating frequency. After thorough consideration, the substrate of 0.508-mm-thick RT/duroid 5880 is used to fabricate the proposed MCCPW structure.

The experiment is conducted combining the proposed IMS and joint feeding network for demonstrating the feasibility of the MCCPW. TRL calibration is used in the following back-to-back circuit measurements to de-embed the test fixture effect. Since all the measurements are carried out on a back-to-back circuit, it means the measured insertion loss consists of the losses in microstrip line part, MCCPW part and transition part. The measurements are carried out using the vector network analyzer N5244A.

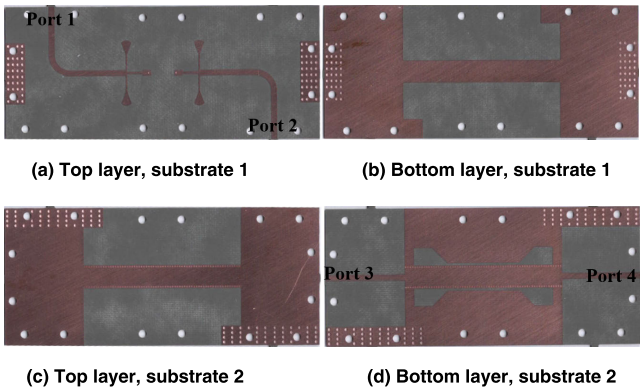

FIGURE 17. Photographs of the fabricated MCCPW with joint feeding network. (a) Top layer, substrate 1. (b) Bottom layer, substrate 1. (c) Top layer, substrate 2. (d) Bottom layer, substrate 2.

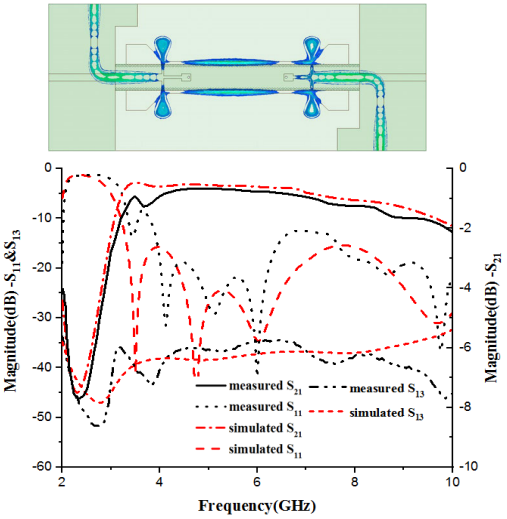

FIGURE 18. Simulated E-field distribution at 5 GHz (top), and simulated and measured S-parameter of MCCPW MCCPW with IMS for low-frequency operation.

A. MCCPW WITH JOINT FEEDING NETWORK

The fabricated MCCPW with back to back joint feeding network is shown in Fig.17. It contains two substrate layers, and two substrates are laminated together using fixing screws. The metallic vias near the feeding point are used to ensure its grounding performance.

During the measurement, when port 1 and port 2 are under test, port 3 and port 4 are terminated by the broadband matching impedance and vice versa as shown in Fig.16. The measured and simulated results of the MCCPW with joint feeding network are shown in Fig.18 and Fig.19. For this feeding technique, two transmission modes are excited separately. The two-mode operation shows very high isolation because of the physical isolation between the ports.

The simulation and measurement results agree well with each other. The TEM mode operates in the QCPW when port 1 is excited. The bandwidth of transition in low frequency can cover 3.2-8GHz with good insertion loss under 1.2dB and reflection coefficient below −15dB. In its high operation band, the SIW TE_{10} mode will work as its fundamental mode.

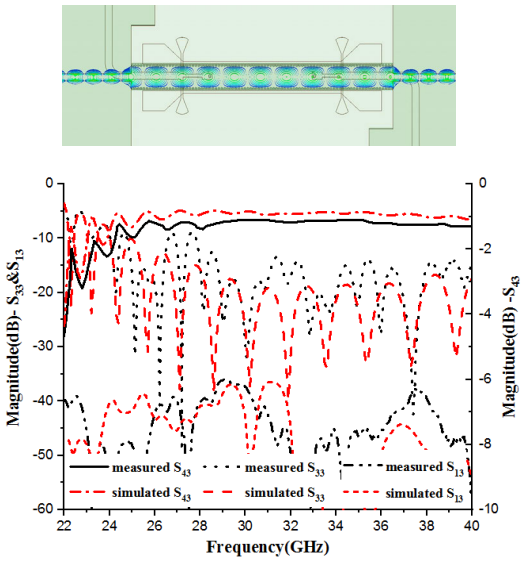

FIGURE 19. Simulated E-field distribution at 28 GHz (top), simulated and measured S-parameter of MCCPW with IMS for high-frequency operation.

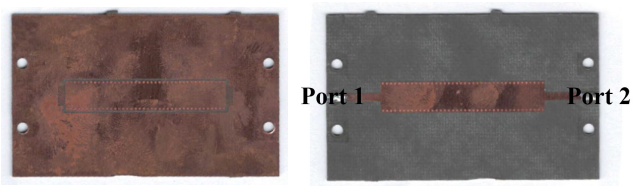

FIGURE 20. Photographs of the top layer (left) and bottom layer (right) of the fabricated MCCPW with back to back IMS.

When the port 3 is excited, the operation band starts from 25GHz with the insertion loss about 1dB and the reflection coefficient under −15dB. When the port 1 and port 3 are excited simultaneously, the two modes will operate within their regions without affecting each other.

B. MCCPW WITH IMS

The fabricated MCCPW with IMS is shown in Fig.20, where the metal width of the center conductor is slightly extended to meet the metallization requirement in practical fabrication. As shown in Fig.21, the simulated and measured results in low frequency are in good agreement. The MCCPW will work in the sub-6GHz band (0-5.2GHz) with the return loss under −15dB and the insertion loss less than 1dB. In this frequency range, the microwave signal is propagating only in the QCPW structure. The bandwidth of the QCPW mode can cover the traditional mobile communication system and the forthcoming 5G mobile communication system at its low operating frequency band according to the existing report.

Fig.22 shows the measured and simulated results of MCCPW with IMS in high operating frequency. The simulation and measurement results agree well in the desired range of frequency from 25GHz to 40GHz. In the high-frequency, the microwave signal is propagating only inside the SIW part of the MCCPW.

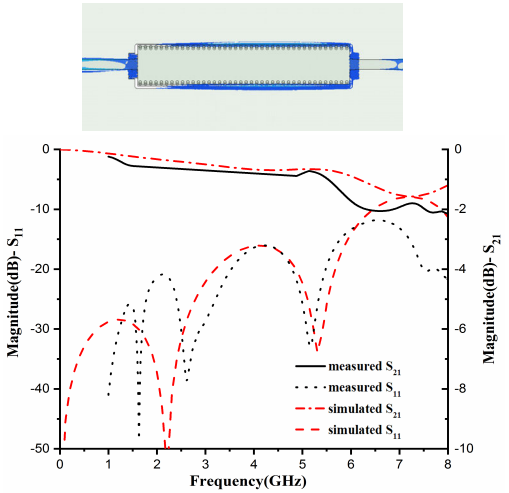

FIGURE 21. Simulated E-field distribution at 3.5 GHz (top), and simulated and measured S-parameter of MCCPW with IMS for low-frequency operation (bottom).

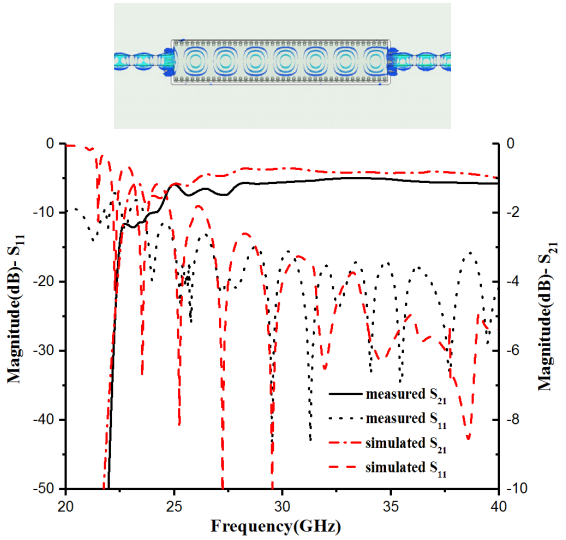

FIGURE 22. Simulated E-field distribution at 32 GHz (top), and simulated and measured S-parameter of MCCPW with IMS for high-frequency operation (bottom).

The full band transmission performance is presented in Fig.23. It shows a suppression at the frequency between 15GHz to 21GHz; the characteristic can help to suppress some of the high order harmonics of the low band. The measurement result is in good agreement with the simulated result.

In this design, the MCCPW is excited and terminated by the microstrip line. So, it can be easily integrated with other planar microwave circuits due to the versatility of the microstrip line. For the MCCPW with IMS, it can support two transmission modes together and can switch the modes to vary the frequency. In the MCCPW with joint feeding network, the two modes can be excited separately. The two feeding techniques make MCCPW easy to integrate with other planar transmission lines and the bandwidth for each feeding technique possesses a broadband characteristic compared

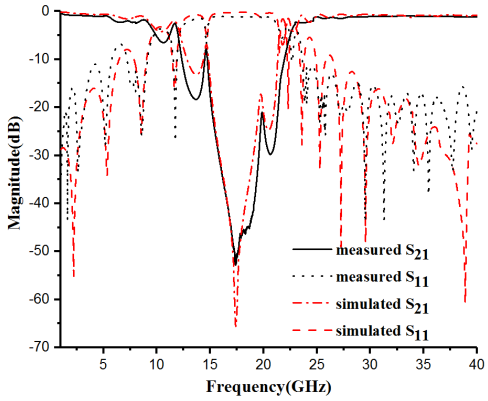

FIGURE 23. Full band simulated and measured S-parameter of MCCPW with IMS.

TABLE 2. Comparison of different Mode Composite transmission line transition structure.

Transmission line type	Substrate Layer	Feeding technique	Low band (RL<-15dB)	High band (RL<-15dB)
MCW [1]	3	Joint feeding	8-10.3GHz (25%)	27-37GHz (31.3%)
MCW [25]	3	Joint feeding	7-11.8GHz (51%)	14-23GHz (48.6%)
DMCMS [7]	2	Joint feeding	3.5-12GHz (109%)	35.6-41.6GHz (15.5%)
MCCPW	**2**	**Joint feeding**	**3-10GHz (108%)**	**25-40GHz (>77%)**
MCCPW	**1**	**IMS**	**0-5.2GHz**	**25-40GHz (>77%)**

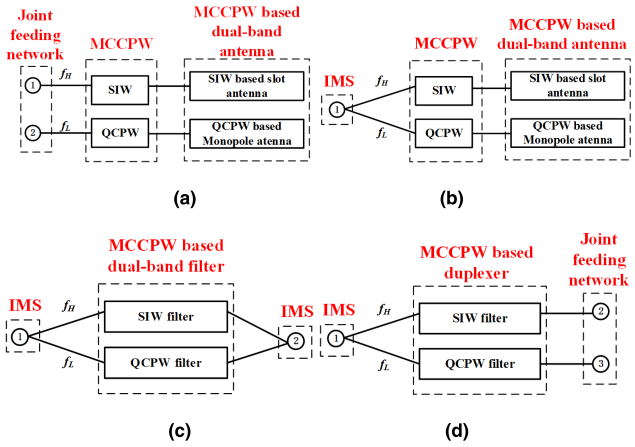

FIGURE 24. Application diagram of the MCCPW together with its transition structure. (a) MCCPW based dual-band antenna with two feedings (b) MCCPW based dual-band antenna with single feeding (c) MCCPW based dual-band filter (d) MCCPW based dulplexer.

with the existing mode composite transmission lines. Table II lists the comparison of the transition structure of different types of mode composite transmission line to demonstrate its superiority.

The future application of the MCCPW is shown in Fig.24 targeting at miniaturized multi-frequency microwave circuits and antennas. And the design freedom of the dual-band

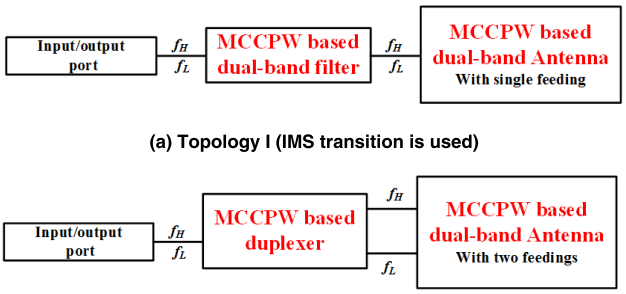

FIGURE 25. MCCPW based circuits and antennas in microwave (f_L) and millimeter-wave (f_H) application. (a) Topology I (IMS transition is used). (b) Topology II (both IMS transition and joint feeding structure).

circuits and antennas is high due to the high isolation of the two modes in the MCCPW. The SIW part of the proposed MCCPW can use the traditional design method to design the microwave circuit such as filter, power divider, antenna, etc. without any restriction. The CPW part can also be applied to the microwave circuits design only to protect the structure of the SIW part from damage.

And due to the large frequency ratio of the two transition structures, the MCCPW based circuits and antenna will be a promising solution for 5G-system in its sub-6GHz and millimeter wave application. Particularly in widely used wireless communication standards such as 802.11 a/b/g, it requires the signals with different frequencies should be transmitted through the same signal chain [25]. In this case, the MCCPW based circuits and antennas will be a good choice, the diagram of the microwave and millimeter-wave application of the MCCPW under the 802.11 a/b/g standards is shown in Fig.25.

VII. CONCLUSION

In this paper, the MCCPW is proposed, which combines the quasi-CPW and SIW techniques in a very compact way with single layer structure; this can make full use of their own advantages, including zero cutoff frequency (CPW), low transmission loss (SIW), broad operating bands, etc. These two constituent parts can selectively operate in different frequency ranges with high isolation. The SIW part supporting the TE_{10} mode as its fundamental mode while The TEM mode signal is transmitted in QCPW part. The single-layer joint structure and mode separation characteristics of MCCPW make it possible in the multifunction and multiband microsystems application. The characteristics are analyzed for the transmission line. Two transition structures are proposed to solve the interconnection problem between the MCCPW and other types of transmission lines. The measured and simulated results are in good agreement which demonstrates the feasibility and practicality of the proposed MCCPW. The future application for the MCCPW is promising as it can combine the feature of SIW and CPW to form more multifunctional small size microwave circuits in microwave and millimeter-wave multi-band system application.

REFERENCES

[1] J. Guo, T. Djerafi, and K. Wu, "Mode composite waveguide," *IEEE Trans. Microw. Theory Techn.*, vol. 64, no. 10, pp. 3187–3197, Oct. 2016.
[2] M. Bozzi, A. Georgiadis, and K. Wu, "Review of substrate-integrated waveguide circuits and antennas," *IET Microw. Antennas Propag.*, vol. 5, no. 8, pp. 909–920, Jun. 2011.
[3] D. Deslandes and K. Wu, "Integrated microstrip and rectangular waveguide in planar form," *IEEE Microw. Wireless Compon. Lett.*, vol. 11, no. 2, pp. 68–70, Feb. 2001.
[4] H. J. Tang, W. Hong, Z. C. Hao, J. X. Chen, and K. Wu, "Optimal design of compact millimetre-wave SIW circular cavity filters," *Electron. Lett.*, vol. 41, no. 19, pp. 1068–1069, Sep. 2005.
[5] M. Abdolhamidi and M. Shahabadi, "X-band substrate integrated waveguide amplifier," *IEEE Microw. Wireless Compon. Lett.*, vol. 18, no. 12, pp. 815–817, Dec. 2008.
[6] D. Deslandes and K. Wu, "Substrate integrated waveguide leaky-wave antenna: Concept and design considerations," in *Proc. IEEE Asia–Pacific Microw. Conf.*, Suzhou, China, Dec. 2005, pp. 1–4.
[7] Y. Li and J. Wang, "Dual-band leaky-wave antenna based on dual- mode composite microstrip line for microwave and millimeter-wave applications," *IEEE Trans. Antennas Propag.*, vol. 66, no. 4, pp. 1660–1667, Apr. 2018.
[8] F. Xu and K. Wu, "Guided-wave and leakage characteristics of substrate integrated waveguide," *IEEE Trans. Microw. Theory Techn.*, vol. 53, no. 1, pp. 66–73, Jan. 2005.
[9] B. C. Wadell, *Transmission Line Design Handbook*. Norwood, MA, USA: Artech House, 1991.
[10] A. Gopinath, "Losses in coplanar waveguides," *IEEE Trans. Microw. Theory Techn.*, vol. MTT-30, no. 7, pp. 1101–1104, Jul. 1982.
[11] M. Riaziat, R. Majidi-Ahy, and I.-J. Feng, "Propagation modes and dispersion characteristics of coplanar waveguides," *IEEE Trans. Microw. Theory Techn.*, vol. 38, no. 3, pp. 245–251, Mar. 1990.
[12] N. Marcuvitz, *Waveguide Handbook*, vol. 21. Edison, NJ, USA: IET, 1951.
[13] P. R. R. Rao and S. K. Datta, "Estimation of conductivity losses in a helix slow-wave structure using eigen-mode solutions," in *Proc. IEEE Int. Vac. Electron. Conf.*, Apr. 2008, pp. 99–100.
[14] C.-K. Yau, T.-Y. Huang, T.-M. Shen, H.-Y. Chien, and R.-B. Wu, "Design of 30 GHz transition between microstrip line and substrate integrated waveguide," in *Proc. IEEE Asia–Pacific Microw. Conf.*, Dec. 2007, pp. 1–4.
[15] D. Deslandes and K. Wu, "Analysis and design of current probe transition from grounded coplanar to substrate integrated rectangular waveguides," *IEEE Trans. Microw. Theory Techn.*, vol. 53, no. 8, pp. 2487–2494, Aug. 2005.
[16] D. Deslandes, "Design equations for tapered microstrip-to-substrate integrated waveguide transitions," in *IEEE MTT-S Int. Microw. Symp. Dig.*, Anaheim, CA, USA, May 2010, pp. 704–707.
[17] J. B. Knorr, "Slot-line transitions," *IEEE Trans. Microw. Theory Techn.*, vol. MTT-22, no. 5, pp. 548–554, May 1974.
[18] Z. Tao, J. Wang, and Y. Dou, "Design of broadband microstrip-to-CPW transition," *Electron. Lett.*, vol. 50, no. 1, pp. 35–37, Jan. 2014.
[19] Z. Tao, "Broadband transition design from microstrip to CPW," *IEEE Microw. Wireless Compon. Lett.*, vol. 25, no. 11, pp. 712–714, Nov. 2015.
[20] L. Zhu and K. Wu, "Accurate circuit model of interdigital capacitor and its application to design of new quasi-lumped miniaturized filters with suppression of harmonic resonance," *IEEE Trans. Microw. Theory Techn.*, vol. 48, no. 3, pp. 347–356, Mar. 2000.
[21] J. L. Hobdell, "Optimization of interdigital capacitors," *IEEE Trans. Microw. Theory Techn.*, vol. MTT-27, no. 9, pp. 788–791, Sep. 1979.
[22] J.-S. Hong and M. J. Lancaster, *Microstrip Filters for RF/Microwave Applications*. Hoboken, NJ, USA: Wiley, 2004.
[23] L. M. George, Y. Leo, and E. M. T. Jones, *Microwave Filters, Impedance-Matching Networks, and Coupling Structures*. Norwood, MA, USA: Artech House, 1980, pp. 434–497.
[24] J. Guo and K. Wu, "Joint feeding network for mode composite waveguide," in *IEEE MTT-S Int. Microw. Symp. Dig.*, Honolulu, HI, USA, Jun. 2017, pp. 1274–1277.
[25] B. J. Xiang, S. Y. Zheng, H. Wong, Y. M. Pan, K. X. Wang, and M. H. Xia, "A flexible dual-band antenna with large frequency ratio and different radiation properties over the two bands," *IEEE Trans. Antennas Propag.*, vol. 66, no. 2, pp. 657–667, Feb. 2018.

YIHONG SU was born in Xiangtan, Hunan, China, in 1995. He received the B.E. degree in electromagnetic field and microwave technology from the University of Electronic Science and Technology of China, Chengdu, China, in 2016, where he is currently pursuing the Ph.D. degree with the School of Electronic Science and Engineering. His current research interests include mode composite transmission line, dual-band/multi-band micro-wave/millimeter-wave antenna, and passive circuit.

XIAN QI LIN (M'08–SM'15) was born in Taizhou, Zhejiang, China, in 1980. He received the B.S. degree in electronic engineering from the University of Electronic Science and Technology of China (UESTC), Chengdu, China, in 2003, and the Ph.D. degree in electromagnetic and microwave technology from Southeast University, Nanjing, China, in 2008. In 2009, he joined the Department of Microwave Engineering, UESTC, where he was an Associate Professor and a Doctoral Supervisor, in 2011. From 2011 to 2012, he was a Postdoctoral Researcher with the Department of Electromagnetic Engineering, KTH Royal Institute of Technology, Stockholm, Sweden. He is currently a Full Professor with UESTC. He has authored more than 40 scientific journal papers and 20 conference papers, and holds more than ten patents. His current research interests include microwave/millimeter-wave circuits, metamaterials, and antennas.

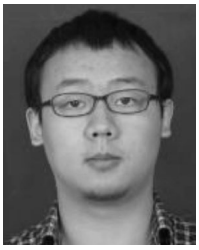

JIA WEI YU was born in Chengdu, Sichuan, China, in 1991. He received the B.S. degree in electromagnetic and wireless technology from the University of Electronic Science and Technology of China, Chengdu, in 2012, where he is currently pursuing the Ph.D. degree in electromagnetic and microwave technology.

YONG FAN received the B.E. degree from the Nanjing University of Science and Technology, Nanjing, China, in 1985, and the M.S. degree in microwave technology from the University of Electronic Science and Technology of China, Chengdu, China, in 1992, where he is currently a Professor and the Dean of the School of Electronic Science and Engineering. His current research interests include millimeter-wave and terahertz technology and systems.